Coupled molecular dynamics and micromechanics study of planar elastic properties of graphene with void defects

Tung Doan, Hung Le Quang, Quy-Dong To

Version of Record: https://www.sciencedirect.com/science/article/pii/S0167663619311317
Manuscript_b96d815dc2a7bf6ada758d82cbf5bb45

Coupled molecular dynamics and micromechanics study of planar elastic properties of graphene with void defects

Tung Doan[a,b], Hung Le-Quang*[a], Quy-Dong To[a,*]

[a] *Université Paris-Est, Laboratoire Modélisation et Simulation Multi Echelle, MSME UMR 8208 CNRS, 5 Boulevard Descartes, 77454 Marne-la-Vallée Cedex 2, France*

[b] *National University of Civil Engineering, No. 55 Giai Phong street, Hai Ba Trung District, Hanoi, Vietnam*

Abstract

In this paper, we employ both molecular dynamics (MD) and micromechanics approach to analyze the influence of void defects on the overall 2-dimensional (2D) elastic behavior of graphene. In the micromechanics model (MM), the edge boundary is assumed to have distinct longitudinal elastic stiffness property (Gurtin-Murdoch model) which can be identified by MD simulations of pristine graphene sheet. Both the Finite Element Method (FEM) and MD are used to study the Eshelby problem involving polygonal nanovoids periodically embedded in a graphene sheet. To characterize the heterogeneity effect due to a single nanovoid, we propose to use MD to compute the tensor $\tilde{\mathbb{C}}$ which is the first order expansion of the effective tensor $\mathbb{C}$ with respect to volume fraction f, related to the dilute scheme estimate. It is shown that the MM performs well for voids with large edges and predicts results consistent with the properties of edge structures. However, MM fails for small voids with short edges where the discrepancies are due to the corner effect which can not be accounted for in MM.

Keywords: Graphene, Molecular Dynamics, Eshelby problem, polygonal

*Corresponding authors. E-mail address: quang-hung.le@u-pem.fr, quy-dong.to@u-pem.fr.

nanovoids, edge effect.

1. Introduction

Since the Nobel prize discovery of graphene (Novoselov et al., 2004), the material has been found to possess many extraordinary properties and gained significant scientific attention over the years. With electrical resistivity of order $10^{-6}\Omega cm$ and thermal conductivity of 5000 $Wm^{-1}K^{-1}$ (Balandin et al., 2008), it is the best conductive material at room temperature. Being mechanically 200 times stronger and 5 times harder than steel, it is also the strongest and lightest 2D material.

There have been theoretical and experimental studies on the mechanical properties of graphene. Among a few experimental methods currently available are atomic force microscope (AFM), instrumented nano-intender (INI), and Raman spectroscopy (RS), etc. The capacity of these methods is limited to the indirect estimation of the elastic modulus of a tiny graphene flake. Properties of larger scale graphene membrane and other mechanical properties, e.g. Poisson's ratio, edge elastic constants, residual stresses, are not accessible. In this case, numerical methods e.g. Ab-initio, Molecular Dynamics (MD), Density function theory (DFT), Molecular Mechanics (MM), Tight Binding (TB), etc. are useful and can provide more direct estimates. However, like experiments, the results reported in the literature are scattering, for example the Young modulus can vary from 0.4 to $4.2TPa$ (Shen et al., 2010; Cao, 2014; Memarian et al., 2015). It is known that the numerical results depend considerably on the computation methods, the techniques used and simulation conditions which are not the same in the previous works. Another distinct feature of graphene is that there are two main directions Armchair (AC) and Zigzag (ZZ) (see Figure 1) and the elastic properties along those two directions can be different (Scarpa et al., 2009; Pei et al., 2010; Gao and Hao, 2009).

In general, atoms near the free boundary behave differently from the bulk

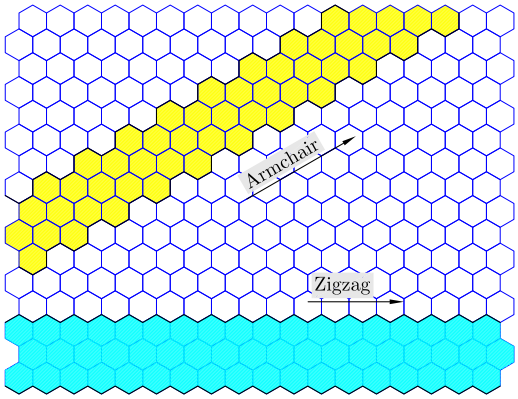

Figure 1: Zigzag and Armchair directions

due to the difference in mobility, coordination number, and potential energy, etc. At large scales, this surface effect is dominated by bulk behavior and is not observable. However, at the nano-scale, it has been proved by experiments and atomistic simulations that this effect is considerable (Cammarata, 1997; Gibbs, 1906; Shuttleworth, 1950; Nix and Gao, 1998) and resulting in the size-dependent behavior. In the case of graphene, edge effects have been studied in several researches. Using MD simulations, Reddy et al. (2009) reported the edge elastic constants are 147.1556 eV/nm for ZZ direction and 112.6304 eV/nm for AC direction. It is also stated in their paper that the edge elastic modulus E_e can vary from -294 eV/nm to 353 eV/nm depending on the edge structures. By similar approach, Lu et al. (2011) found the results are 52 eV/nm for ZZ edge and 23 eV/nm for AC edge. For AC direction only, Li et al. (2015) reported negative values of edge elastic modulus from $-64N/m$ to $-47N/m$. Despite the wide range of existing results, currently there is no experiment method to directly measure this constant of graphene membranes to confirm those values.

Like all materials, defects are unavoidable in the synthesis process of graphene. There are several kinds of structural defects can happen and they can be

classified into three main groups: vacancy defects, adatoms, and atom reconstruct defects (Banhart et al., 2010). Wang et al. (2015) studied the effects of 5-8-5 defects on graphene and stated that, comparing with the elastic modulus of pristine graphene, the stiffness of defected graphene in the AC direction is smaller, where that of graphene in ZZ direction becomes larger. By using the TB method, Dettori et al. (2012) studied the elastic moduli of graphene with vacancy and various reconstructed defects and concluded that the important factor that affects the elasticity of defected graphene is the changing in the absolute mass density, not the types of the reconstruction of the atoms. This conclusion is also supported by (Ansari et al., 2012). In this work, we are interested in vacancy defects which is one of important factors that affect the mechanical properties of graphene.

At continuum scale, micromechanics method is known as an analytically accurate and efficient approach to predict the effective properties of heterogeneous materials in general and porous materials in particular. The theoretical framework of the approach is well founded in literature (see e.g Mura, 1987; Milton, 2002; Torquato, 2001, and the references therein). One of the standard techniques in micromechanics, is to study the Eshelby inclusion problem (Eshelby, 1957) in which a single inclusion (or void) is embedded in an infinite matrix and subjected to an uniform loading at infinity. From this elementary solution, estimates for mixtures of inclusions at finite volume fraction f can be derived using relevant schemes, e.g dilute, Mori-Tanaka, self-consistent schemes, etc.. Since the original Eshelby's inclusion problem is devoted to an ellipsoidal inclusion, for nanovoids, it is necessary to introduce the edge effect in the micromechanics model. In many cases, using the elastic Gurtin-Murdoch (GM) edge model (Gurtin and Murdoch, 1975) can produce satisfactorily these edge effects. The Eshelby inclusion problem involving 2D polygonal nanovoids like graphene and using GM model have been studied recently in (Doan et al., 2020). While all those works are

based on the continuum mechanics, it can not capture all the behavior at the atomic scale, especially when there is variation of atomic structure along the void edges or interaction of atoms across the edges etc... The heterogeneity effect due to those factors are complex and can affect the accuracy of stiffness estimates. Most literature works based on MD methods (see e.g Rafiee and Eskandariyun, 2017; Savvas and Stefanou, 2018) are more concerned about the effective properties of the graphene with voids without relating to the local behavior of voids. This motivates us to investigate the Eshelby problems under the micromechanics framework and characterize the void defects of graphene using both MD and continuum based methods in the present paper.

The paper will be organized as follows. First, we describe the general framework and procedure to find the elastic properties of graphene, including the edge elastic constants (Sec. 2) and graphene sheet with voids using MD simulations. Next, in Sec. 3, we carry out coupled MD-MM studies on graphene with nanovoids. The MD results are compared with the MM results based on FEM analysis using the bulk and the edge elastic properties obtained from previous steps. The objective of the comparisons is to investigate the impact of edge effects on the overall properties. Finally, some concluding remarks are given in the last section.

2. Determination of bulk and edge stiffness of graphene

At atomic scale, MD is an efficient computation method for studying the motion of atoms and determining the macroscopic properties of materials by statistical averages. We use an open source code LAMMPS (Plimpton, 1995) to run our MD simulation due to its computational efficiency and parallel capacity. The Adaptive Inter-molecular Reactive Empirical Bond Order (AIREBO) potential by Schall et al. (2012) which is relevant to simulate Carbon system like graphene, was used in the study. As mentioned previously,

due to various reasons, the values of the bulk and edge stiffness reported in literature are scattering. To keep the consistency, we use the same computation method and simulation conditions throughout the present paper and devote this section to determine those constants with the method. In addition to the simulation conditions, the definition of geometric boundary of graphene sheet can also affect the computed values and will be discussed.

Temperature is known to have effects on the elastic modulus of graphene. The Young modulus of graphene drops approximately 10% when the temperature increases from 1 to 1200K (Zhang et al., 2014). Under finite temperature, multiple complex phenomena associated to the out-of-plane behaviors like rippling, bending, buckling, vibration etc.. can appear and interact with the in-plane behavior. Consequently, the computation results obtained under such conditions have very high uncertainty and vary significantly. Due to the ripples, the tension and compression stiffness can be different (Sgouros et al., 2018) and depend on the sample size (Los et al., 2016). It is suggested that those issues can be addressed based on out-of-plane flexible plate and membrane models (see e.g Fasolino et al., 2007; Wang et al., 2009). In the present study of planar elastic stiffness, we do not consider the rippling phenomenon and maintain the system in the plane (see e.g Arroyo and Belytschko, 2004; Saavedra Flores et al., 2015; Marenić et al., 2013; Lu and Huang, 2009; Jiang et al., 2010; Wei et al., 2009; Javvaji et al., 2016) at temperature as low as 10K. The thickness of the system in z direction is taken as 3.4 Å. In the strain control simulation, the system is stretched (direct strain ϵ_1 or ϵ_2 imposed) or tilted (shear strain ϵ_3 imposed) on its periodic boundaries. After applying a small strain level (order 0.1%), the system was relaxed for the next 8e5 timesteps of 0.001ps to achieve the equilibrium NVT state where time and sample average of system properties can be computed. For example, in this case, we are interested in the average potential energy of the system at each strain value. At small strain and temperature, the graphene

can be considered as linear elastic material and the potential energy density U is quadratic function of strain. Here, we assume that at temperature as low as 10K, the strain energy can be assimilated to the potential energy and the variation of the latter govern the elastic behavior of the nanosystem. By fitting the potential energy with quadratic functions of strain components, stiffness constants can be derived. The method can be applied to compute the properties for any systems with periodic boundaries along x- and/or y-directions of pristine graphene or graphene with defects, as described in the following.

To compute the bulk stiffness constant of graphene, we use a sufficiently large graphene sheet with periodic boundary conditions along x- and y-directions and impose strain on the plane xy as described previously. We can write using the Voigt's notation:

$$U = U_0 + U_1 + U_2, \tag{1}$$

$$U_0 = \text{cste}, \quad U_1 = \sigma_i^0 \epsilon_i, \quad U_2 = \frac{1}{2} C_{ij} \epsilon_i \epsilon_j \tag{2}$$

where σ_i^0 is the residual stress, C_{ij} the elastic constants and U_0 the potential energy at the reference strain free state. Specifically, the quadratic form of U_2 can be written explicitly as follows

$$U_2 = \frac{1}{2}(C_{11}\epsilon_1^2 + 2C_{12}\epsilon_1\epsilon_2 + 2C_{13}\epsilon_1\epsilon_3 + C_{22}\epsilon_2^2 + 2C_{23}\epsilon_2\epsilon_3 + C_{33}\epsilon_3^2) \tag{3}$$

For example, to find the elastic constant C_{11} (or C_{22} and C_{33}), it is sufficient to vary the strain $\epsilon_1 = \epsilon$ and maintain the other strain components at zero value $\epsilon_2 = \epsilon_3 = 0$. In this case, U becomes

$$U = \frac{1}{2} C_{11} \epsilon^2 + \sigma_1^0 \epsilon + U_0 \tag{4}$$

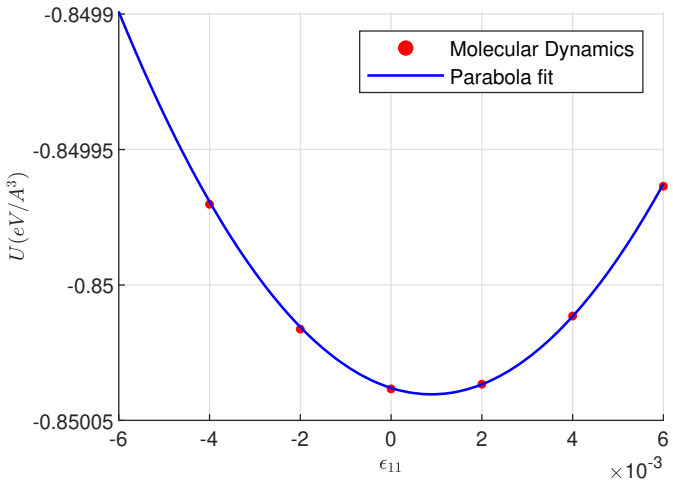

Figure 2: Potential energy U as function of strain $\epsilon_1 = \epsilon$. The parabola fitting of MD results is used to determine C_{11}^b.

As a result, if we have sufficient number of potential energy - strain (ϵ, U) points from MD simulations, it is possible to identify the elastic constants C_{11} by parabola fit (see Fig. 2). To determine C_{12}, we apply simultaneously the same amount of direct strain $\epsilon_1 = \epsilon_2 = \epsilon$ along both 1 and 2 direction. In this case, Equation 3 becomes

$$U = \frac{1}{2}(C_{11} + 2C_{12} + C_{22})\epsilon^2 + (\sigma_1^0 + \sigma_2^0)\epsilon + U_0 \tag{5}$$

The procedure of computing the hybrid coefficients $C_{11} + 2C_{12} + C_{22}$ associated to ϵ^2 is the same as before. With C_{11} and C_{22} already known from the previous step, we can solve for C_{12}.

When applying the above method to pristine graphene, we obtain the bulk elastic stiffness of graphene C_{ij}^b. The elastic modulus E_b and the Poisson's ratio ν for isotropic materials are computed from:

$$E_b = C_{11}^b(1 - \nu_b^2), \quad \nu_b = \frac{C_{12}^b}{C_{11}^b}. \tag{6}$$

Results from MD simulations of system 96.7 Å x 96.3 Å containing 3680 atoms, give the values of $C_{11}^b = C_{22}^b = 953$ GPa and $C_{12}^b = 323$ GPa respectively. Consequently, the matrix elastic modulus E_b and the Poisson's ratio calculated from Eq. 6 take the values 843.8 GPa and 0.338 respectively. These values are very close to literature results (Pei et al., 2010; Terdalkar et al., 2010; Tu and Ou-Yang, 2002).

To determine the edge stiffness E_e of graphene, we need to consider a system with free surfaces. This is the case of graphene nanoribbon (GNR) where we apply strain along its length l, the periodic direction, and the width w direction is free of stress. It is necessary to account for both bulk energy density U_b uniform for the whole volume wl and edge energy U_e, i.e energy localized along the two edges of length l, as follows

$$wlU = wlU_b + 2lU_e \tag{7}$$

The dependency of those two quantities on prescribed strain ϵ is given by

$$U_b = \frac{1}{2}E_b\epsilon^2 + \sigma_1^0\epsilon + U_{b0}, \quad U_e = \frac{1}{2}E_e\epsilon^2 + \tau_1^0\epsilon + U_{e0}, \tag{8}$$

where σ_1^0, τ_1^0 respectively are the residual stresses in the bulk and in the edges, and U_{b0}, U_{e0} are the potential energies at the reference zero strain state in the bulk and in the edges respectively.

One can find that the effective Young modulus of the GNR can be determined as

$$E = E_b + \frac{2}{w}E_e.$$

Since E for a given GNR can be determined from U using the same procedure as before (replacing E for C_{ii}), doing tests with different width values w will

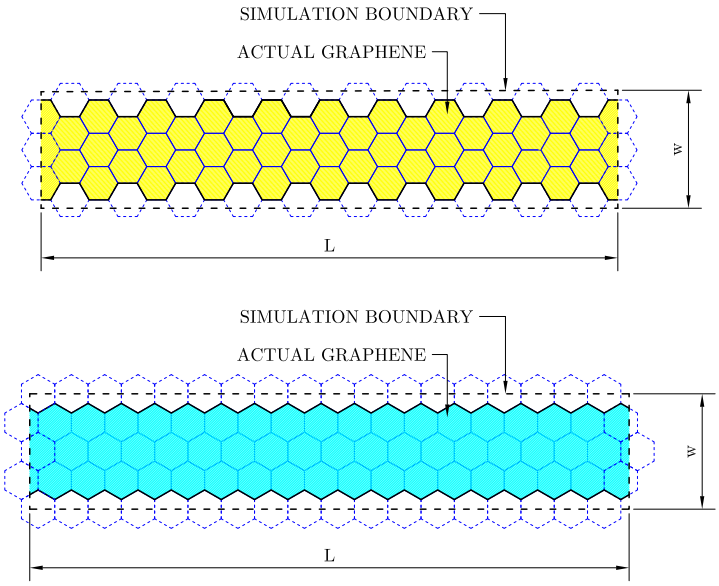

Figure 3: Continuum boundary and width w of GNR. Top: GNR with AC edges, Bottom: GNR with ZZ edges.

generate data to find E_e and E_b. We note that the width w determined from the volume of the GNR is different from the geometric distance of extreme atoms belonging to the two opposite edges (see Fig. 3). While the latter definition can be used to analyze the behavior of pristine graphene, it is not relevant for the study of nanovoids where the void volume fraction f must be defined as well. To guarantee the consistent volume definition throughout the paper and the conservation of volume, we consider that each atom occupies the same volume and the volume of graphene objects is proportional to the number of atoms contained inside. For example, if the number density of graphene is denoted as n, the area (or volume) of a graphene sheet composed of N carbon atom is equal to $V = nN$ and the width $w = V/L$ where L is the length of the graphene sheet. This definition will affect the width of the graphene sheets and consequently the value of edge stiffness when fitting MD results with continuum models. In the GNR simulations, the length of the ZZ ribbons are 67.7 Å while the width is changing from 16.7 Å to 100.5 Å. For

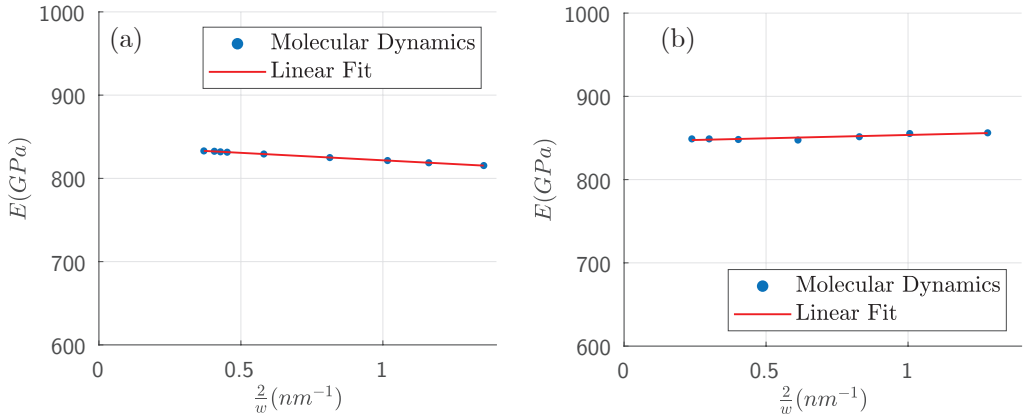

Figure 4: Effective Young modulus of GNR as function of inverse width w^{-1}. The linear fitting is used to find E_b and E_e (a) AC direction (b) ZZ direction.

AC ribbons, the length is 83.76 Å and the width is from 14.5 Å to 53.19 Å. From Fig. 4, we find that E varies linearly with the inverse width w^{-1} but differently for AC and ZZ directions. The slopes can be used to compute the edge elastic constants E_e in each direction and the intersections with the vertical axis give E_b. The GNR simulations yield the values $E_b = 842\, GPa$ for both directions, close to the value 843.8 GPa determined from the previous periodic systems. The edge elastic modulus E_e is found 11.9 $GPa.nm$ for ZZ direction and -17.9 $GPa.nm$ for AC direction, or 25.62 eV/nm and -38.54 eV/nm respectively. Since the stiffness of graphene can be considered as the contribution of the bulk and the edge, the ZZ edges with positive stiffness tend to stiffen and AC edges with negative stiffness soften the graphene. For the same void shape and size, graphene with ZZ edges is stiffer than graphene with AC edges. From the ratio E_e/E_b, it is suggested that for objects of size 1-2 nm, the difference due to the free edge is of order 1-2%. The difference can be more pronounced for objects of sub nanometric size. We note that due to the lattice structure of graphene, the characteristic size of objects cut from a pristine graphene sheet is limited by the lower bound value 1.42 Å. Furthermore, the above determination of E_e is done on infinitely long GNR,

which may be not valid for systems containing short edges. In this case, the local interaction of atoms at corners may also be important and affect the global behavior of the system.

3. Characterization of void effect in graphene

To investigate the void size and shape effects on the stiffness of the graphene, we run MD simulations of graphene sheets with different types of voids and use the same method described in Section 2 to calculate the effective properties of the system. Results are then compared with the continuum models (with and without edge effect), solved by the FEM. Comparisons are performed on the problem of periodic cell with single void. Like the volume of graphene, the void volume V_{void} is computed from the number density n of graphene and the number of missing carbon atoms N_{void} via the relation $V_{void} = nN_{void}$. We also denote $f = V_{void}/V$, as the volume fraction of the void (or porosity), an important quantity to evaluate the effective properties of porous material. In the case where $f \to 0$, we shall recover the Eshelby problem with a void in an infinite matrix. In the FEM models (Fig. 5), the cell dimensions are the same as those in the MD model. The bulk is isotropic with $E_b = 842$ GPa and $\nu_b = 0.338$ and the edge effect is modeled by a thin material layer with thickness t and elastic constant $E_{layer} = E_e t$ (Shenoy et al., 2008). In the ideal case where $t \to 0$, it can be shown theoretically that the Gurtin-Murdoch model can be recovered (Benveniste and Miloh, 2001; Hashin, 2002; Benveniste, 2006). In practical FEM applications, t should not be too small to avoid mesh issues and chosen as $t = 0.005\,\text{Å}$ (Doan et al., 2020). Different void shapes including diamond, hexagon, narrow rectangle (crack like) constituted by different edge structures like pure AC edges, pure ZZ edges (Figures 6, 8) and mixed AC and ZZ edges (Figure 7) are considered in this work. The effective stiffness $\mathbb{C}$ of the graphene sheet with voids under periodic boundary conditions is determined using the method in Section 2.

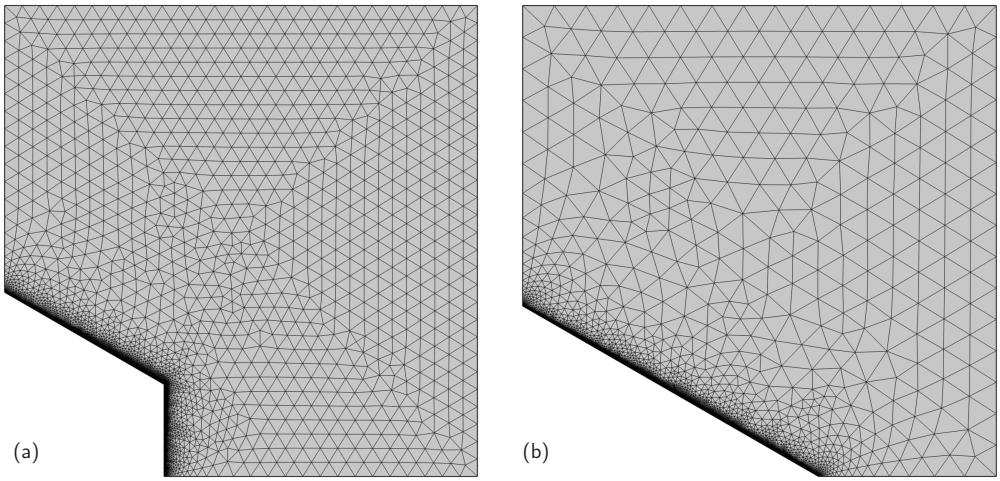

Figure 5: Finite element meshes of graphene sheet containing different types of voids (a) Hexagon (b) Diamond.

In addition to the effective stiffness $\mathbb{C}$ of graphene, we are also interested in the quantity $\tilde{\mathbb{C}}$

$$\mathbb{C} = \mathbb{C}^b + f\tilde{\mathbb{C}} + O(f^2), \quad \text{or} \quad \tilde{\mathbb{C}} = \lim_{f\to 0} f^{-1}(\mathbb{C} - \mathbb{C}^b) \tag{9}$$

This tensor $\tilde{\mathbb{C}}$, equivalent to the first order expansion of $\mathbb{C}$ with respect to f, is both useful for MD and continuum models for the evaluation of nanovoid contribution in the effective stiffness. For the latter case, it corresponds to the limit of dilute and Mori-Tanaka (MT) scheme at a small f, related to the localization tensor and the equivalent stiffness of the nanovoid (see Appendix Appendix A for more details). It is noted that the MT estimate is based on solutions of heterogeneity problems involving single nanovoid in infinite matrix. The solutions can be obtained using the Conformal Mapping techniques proposed by previous works (Doan et al., 2020). Due to a large number of simulated systems in the present paper, we shall focus on the comparison

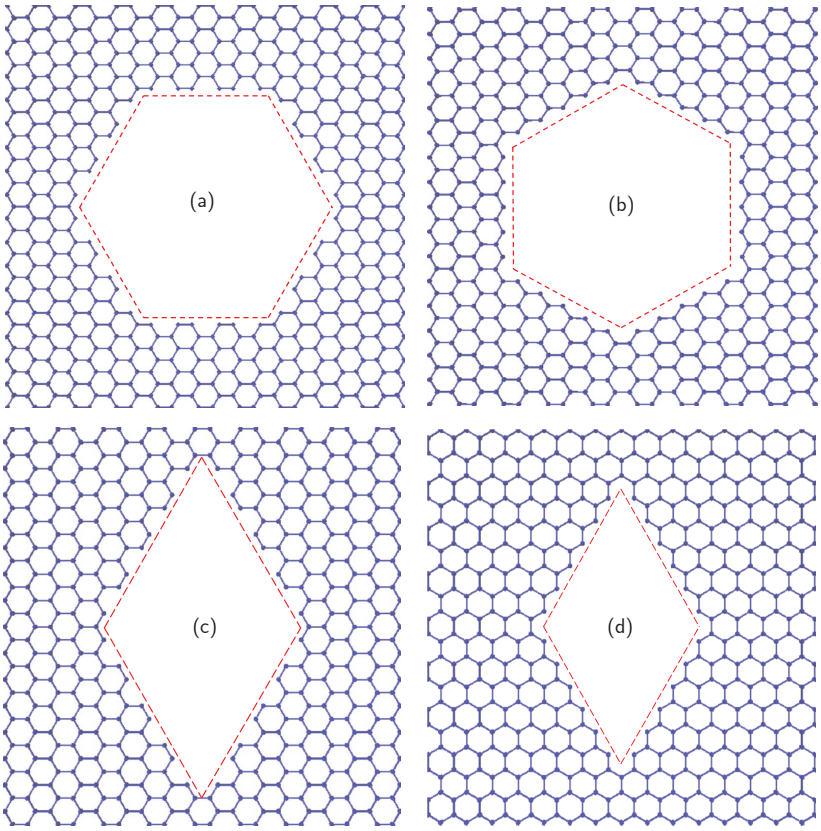

Figure 6: Typical void shapes and edge structures (a) Hexagon AC edge (b) Hexagon ZZ edge (c) Diamond AC edge (d) Diamond ZZ edge.

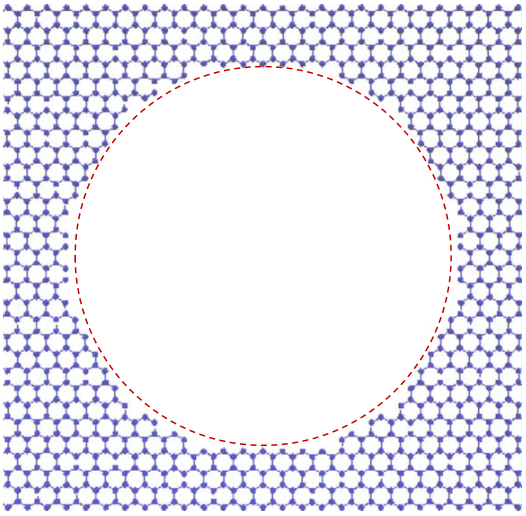

Figure 7: Circular void shape with mixed edge structures.

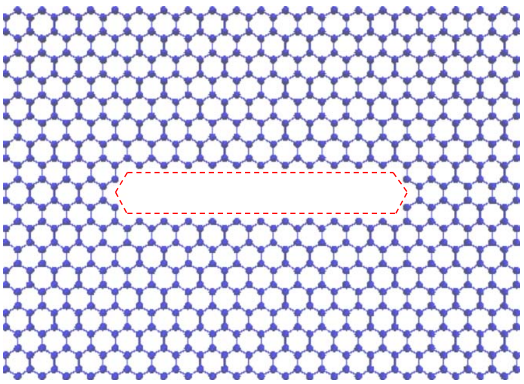

Figure 8: Cracked graphene with ZZ edge structures.

of the representative stiffness components C_{11} and C_{22} of the elastic tensor $\mathbb{C}$.

First, we take the pristine graphene system of 3680 atoms and remove the atoms at the center to obtain the desired void size and shape. The results for each kind of voids with different sizes are shown in Tables 1 and 2. In these tables, FEM^1 and FEM^2 are the results from FEM models with and without edge effects respectively. We can see the edge effects on the elastic stiffness of the voids and the graphene sheet. As expected, for the case of ZZ edge voids with positive edge elastic modulus, the graphene cell is stiffened, and for AC voids, due to the negative stiffness, the effective elastic modulus decreased. For mixed edges void, the edge elastic constant in AC and ZZ are in opposite signs and the overall edge effect can be considered canceling out each other. For the pure AC or ZZ edge structure, the continuum models with edge behavior are in excellent agreement with MD results and perform slightly better than models without edge behavior. The difference due to the edge effect is relatively small for large edge due to the small ratio of E_e/E_b as mentioned previously. Since the size of the cell is fixed, it can be seen that the effect of edge structures decreases when the graphene area decreases. This fact agrees with the statement concluded by Dettori et al. (2012) previously mentioned.

However, from the micromechanics viewpoint, the effective behavior can be dominated by the bulk which has significant volume fraction and masks the local behavior of the nanovoid. We note that due to the void shape and the atomic structure, in most of the simulated cases, the maximal achievable volume fraction f of voids is relatively small, order 0.2. This motivates us to investigate the contribution of the nanovoid only via the tensor $\tilde{\mathbb{C}}$, which is independent of volume fraction f and only depends on the void size and shape. We are also looking into the cases of small nanovoids (short edge) and higher volume fraction (small cell) where strong edge and corner effects

can be observable.

We carried out MD simulations where the void size is fixed while the cell size increases. Shown in the Tables 3 and 4 are the results in comparison with FEM models. Like the previous test, we found good agreement between MD simulations and FEM models and MT estimates for most of the considered cases. However, we can see the larger errors between the MD and the continuum models, especially for the case of small void and high volume fraction (order 0.2) including diamond void 8/112 ZZ and hexagon void 24/112 AC. A careful inspection of the $f - C_{11}$ and $f - C_{22}$ slope near the origin $f = 0$ shows that the nanovoid coefficients $\tilde{C}_{11}$ and $\tilde{C}_{22}$ are considerably different between the MD and the continuum models. It implies that the micromechanics approach already fails to solve the heterogeneity problem with acceptable error. The $\tilde{C}_{11}$ and $\tilde{C}_{22}$ errors for the two mentioned cases are of order 20%. It confirms the previous suggestion that due to the small volume fraction, the discrepancies due to the nanovoid effect are masked by the bulk behavior. We note that all the coefficients $\tilde{C}_{11}$ and $\tilde{C}_{22}$ are negative showing that the voids have weakened the graphene, even when ZZ edges with stiffening effect are used. Theoretically, using the ZZ edge hole to stiffen the graphene only works for very tiny hole, for example one atom vacancy defect. This is the case of López-Polín et al. (2015) who found experimentally that it is possible to increase the stiffness of graphene by removing a very small number of carbon atoms.

There is another interesting feature we can observe at small nanovoids. While the use of edge elastic model improves the prediction of micromechanics approach in most cases, the case 24/112 with AC edges shows a reverse trend. There can be a strong corner effect can affect the global behavior. As mentioned previously, the edge model is based on the parameter E_e obtained for infinite long edge. For small nanovoids, the edge is short, with few atoms,

and the number of corner atoms is comparable with edge atoms. Furthermore, atoms belonging to different edges near the common corner can interact within the interaction range (see Fig. 9) and it is difficult to distinguish edge and corner atoms. This corner effect seems to stiffen the hole and cancel out the softening effect of AC. As a result, the overall behavior of graphene shows that the model without edge model performs better. To capture the corner effect with micromechanics approach, we need a special model devoted to the corner. We note that similar ideas based on cohesive crack or adhesive contact models accounting for van der Waals interaction forces at the interface can be useful in this case and will be investigated in the future.

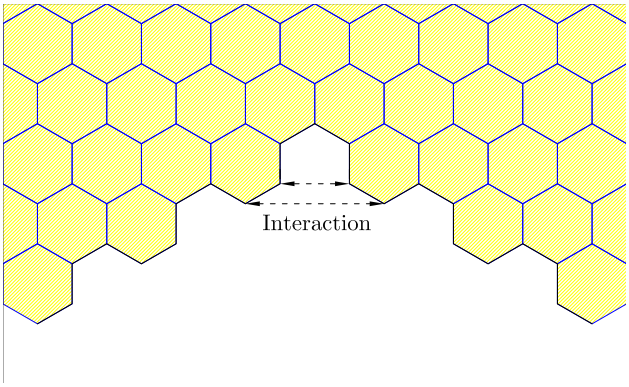

Figure 9: Interaction between atoms around corner

Another issue of nanovoid that limits the application of micromechanics model is when the vacancy defects are reduced to several atoms. It is difficult to detect the clear edge structure and construct the geometry of micromechanics model. In this case, the present MD based approach can also address the problem. Especially, the determination of the nanovoid tensor $\tilde{\mathbb{C}}$ is always feasible. This tensor, which is independent of the volume fraction, can provide insight into the local behavior of the nanovoid by including both corner and edge effects.

Void/Cell(atoms)	f	MD	FEM^1	FEM^2
Diamond void - AC edges				
16/3680	0.004	936.6	940.1	940.9
112/3680	0.03	829.7	834.7	837.0
294/3680	0.08	779.6	782.7	784.0
560/3680	0.152	655.3	661.9	667.7
726/3680	0.197	600.1	602.1	606.5
Diamond void - ZZ edges				
72/3680	0.020	908.0	906.8	905.0
128/3680	0.035	874.6	874.2	871.8
200/3680	0.08	834.7	834.7	831.8
288/3680	0.078	789.2	798.8	786.5
392/3680	0.107	740.3	741.0	737.5
512/3680	0.139	688.8	689.7	686.0
Hexagon void - AC edges				
180/3680	0.049	822.1	818.5	819.9
264/3680	0.072	758.7	768.8	768.4
366/3680	0.099	707.7	705.0	713.0
762/3680	0.207	534.9	533.0	539.0
Hexagon void - ZZ edges				
24/3680	0.007	945.6	932.2	931.3
54/3680	0.015	913.4	909.5	908.2
96/3680	0.026	882.3	879.0	877.3
150/3680	0.041	845.0	842.0	840.0
384/3680	0.104	707.2	706.0	703.3
486/3680	0.132	656.9	656.3	653.6
Circular void - Mixed edges				
258/3680	0.070	776.4	-	777.8
348/3680	0.095	729.6	-	727.0
450/3680	0.122	678.8	-	674.0
576/3680	0.157	615.0	-	620.0
708/3680	0.192	562.4	-	565.9

Table 1: Effective elastic constant C_{11} in MPa - MD results and solutions from FEM (with and without elastic model)

Void/Cell(atoms)	f	MD	FEM^1	FEM^2
Diamond void - AC edges				
16/3680	0.004	932	927	926
112/3680	0.03	720	705	705
294/3680	0.08	626	614	611
560/3680	0.152	437	422	423
726/3680	0.197	345	331	331
Diamond void - ZZ edges				
72/3680	0.020	845	843	843
128/3680	0.035	774	773	773
200/3680	0.08	695	696	695
288/3680	0.078	613	614	614
392/3680	0.107	530	532	532
512/3680	0.139	449	451	451
Hexagon void - AC edges				
180/3680	0.049	819	822	822
264/3680	0.072	755	768	770
366/3680	0.099	704	714	715
762/3680	0.207	530	533	540
Hexagon void - ZZ edges				
24/3680	0.007	935	934	933
54/3680	0.015	913	912	910
96/3680	0.026	882	881	879
150/3680	0.041	846	844	842
384/3680	0.104	708	707	705
486/3680	0.132	659	658	655

Table 2: Effective elastic constant C_{22} in MPa - MD results and solutions from FEM (with and without elastic model)

	Void/Cell(atoms)	f	MD	FEM^1	FEM^2	MT
			Diamond void - ZZ edges			
C_{11}	8/1232	0.0065	940	939	937	939
	8/448	0.0179	919	915	910	915
	8/240	0.0333	890	884	876	885
	8/112	0.0714	823	815	800	814
$\tilde{C}_{11}$	-	-	-3376	-3671	-4087	-3650
			Diamond void - AC edges			
C_{11}	54/3680	0.015	915	914	915	915
	54/2800	0.019	905	905	906	905
	54/1232	0.044	849	849	853	846
	54/240	0.225	561	559	570	528
$\tilde{C}_{11}$	-	-	-2590	-2658	-2590	-2616
			Hexagon void - ZZ edges			
C_{11}	24/3680	0.0065	936	934	933	935
	24/2800	0.0086	931	929	927	929
	24/1232	0.0195	903	899	897	899
	24/240	0.100	728	722	713	716
$\tilde{C}_{11}$	-	-	-2662	-2870	-3005	-2826
			Hexagon void - AC edges			
C_{11}	24/1232	0.019	901	892	896	893
	24/448	0.054	825	798	808	794
	24/240	0.100	729	696	711	685
	24/112	0.214	553	506	529	482
$\tilde{C}_{11}$	-	-	-2656	-3129	-2914	-3102
			Crack void - ZZ edges			
C_{11}	46/3680	0.0125	926	925	924	926
$\tilde{C}_{11}$	-	-	-2137	-2210	-2308	-2189

Table 3: Effective elastic constants C_{11} and $\tilde{C}_{11}$ in MPa- Comparisons between FEM (with and without edge effect), MD and Mori Tanaka (MT) estimates.

	Void/Cell(atoms)	f	MD	FEM^1	FEM^2	MT
			Diamond void - ZZ edges			
C_{22}	8/1232	0.0065	911	912	11	917
	8/448	0.0179	852	825	851	859
	8/240	0.0333	781	780	778	789
	8/112	0.0714	637	637	634	651
$\tilde{C}_{22}$	-	-	-3322	-3361	-3399	-3255
			Diamond void - AC edges			
C_{22}	54/3680	0.015	860	869	868	865
	54/2160	0.025	841	819	819	812
	54/1232	0.044	784	738	737	727
	54/240	0.225	380	273	275	321
$\tilde{C}_{22}$	-	-	-6359	-5725	-5816	-5973
			Hexagon void - ZZ edges			
C_{22}	24/3680	0.0065	935	934	933	935
	24/2800	0.0086	930	929	927	929
	24/1232	0.0195	903	899	897	899
	24/240	0.100	732	722	713	716
$\tilde{C}_{22}$	-	-	-2760	-2870	-3067	-2760
			Hexagon void - AC edges			
C_{22}	42/1232	0.0341	857	848	857	848
	42/448	0.0938	725	706	724	698
	42/240	0.1750	580	557	585	542
	42/112	0.3750	343	321	353	295
$\tilde{C}_{22}$	-	-	-2824	-3068	-2829	-3085
			Crack void - ZZ edges			
C_{22}	46/3680	0.0125	811	814	812	813
$\tilde{C}_{22}$	-	-	-11374	-11152	-11309	-11187

Table 4: Effective elastic constants C_{22} and $\tilde{C}_{22}$ in MPa- Comparisons between FEM (with and without edge effect), MD and Mori Tanaka (MT) estimates.

4. Conclusions and perspectives

In this work, we study the effective stiffness of pristine graphene and graphene containing nanovoids. The elastic constants of the bulk and the free edges according to the Gurtin-Murdoch model are determined by MD simulation. It is found that the free edge stiffness depends on the edge structure, negative for armchair or positive for zigzag. The continuum-based micromechanics models constituted of graphene and vacancy defects are then constructed using the elastic parameters obtained by MD methods. The effective properties of the defected graphene are computed by different approaches FEM and compared with full MD simulations. In addition to the effective properties of graphene with voids $\mathbb{C}$, the heterogeneity effects due to a single nanovoid are characterized via the tensor $\tilde{\mathbb{C}}$, the first-order expansion of $\mathbb{C}$ with respect to f.

The results issued from the comparisons show that the effective elastic stiffness obtained by micromechanics models and estimates is in good agreement with the MD results and consistent with the softening and stiffening effect of the edge structures. For small nanovoids, we observe larger discrepancies between MD and MM and further inspection of nanovoid coefficients $\tilde{\mathbb{C}}$ show that MM fails to capture the behavior of nanovoids including both edge and corner effects. In some cases, those considerable errors may be masked in the overall behavior due to the small volume fraction of the nanovoid. We conclude that it is necessary to develop models devoted to the sharp corners, not only for graphene but also for nanoporous materials in general, to fully capture the behavior of the nanopores.

Another interesting problem that merits future consideration is to investigate the out-of-plane behavior of graphene. While plate and membrane models can successfully reproduce the behavior of pristine graphene, the influence of the defect heterogeneity combined with the intrinsic ripples on the effective

bending and stretching behaviors needs to be explored and understood.

Appendix A. Relation between the void coefficient $\tilde{\mathbb{C}}$ and the heterogeneity problem with edge effects

Let us consider the heterogeneity problem where a single nanovoid (index v) of edge stiffness E_e is embedded in an infinite matrix of bulk stiffness $\mathbb{C}^b$ subject to remote strain $\mathbf{E}$. Solving the problem will yield the localization tensor $\mathbb{L}^v$ and equivalent elastic stiffness tensor $\mathbb{C}^v$ of the nanovoid as follows

$$\langle \boldsymbol{\varepsilon} \rangle_v = \mathbb{L}^v : \mathbf{E}, \quad \langle \boldsymbol{\sigma} \rangle_v = \mathbb{C}^v : \langle \boldsymbol{\varepsilon} \rangle_v, \tag{A.1}$$

where $\langle \boldsymbol{\sigma} \rangle_v$ and $\langle \boldsymbol{\varepsilon} \rangle_v$ stand for the average stress and strain of the nanovoid and : for double contracted product.

From the results of the above heterogeneity problem, we can estimate the effective elastic stiffness tensor $\mathbb{C}$ of materials containing nanovoids of volume fraction f by Mori-Tanaka scheme

$$\begin{aligned} \mathbb{C} \simeq \mathbb{C}_{\mathrm{MT}} &= \left\{(1-f)\mathbb{C}^b + f\mathbb{C}^v : \mathbb{L}^v\right\} : \left\{(1-f)\mathbb{I} + f\mathbb{L}^v\right\}^{-1} \\ &= \mathbb{C}^b + f(\mathbb{C}^v - \mathbb{C}^b) : \mathbb{L}^v : \left\{(1-f)\mathbb{I} + f\mathbb{L}^v\right\}^{-1} \end{aligned} \tag{A.2}$$

In the case where $f \to 0$, we obtain the asymptotic behavior of dilute scheme

$$\mathbb{C} \simeq \mathbb{C}_{\mathrm{dilute}} = \mathbb{C}^b + f(\mathbb{C}^v - \mathbb{C}^b) : \mathbb{L}^v \tag{A.3}$$

Using the definition of $\tilde{\mathbb{C}}$ in (9), we have

$$\tilde{\mathbb{C}} = (\mathbb{C}^v - \mathbb{C}^b) : \mathbb{L}^v \tag{A.4}$$

References

Ansari, R., Ajori, S., Motevalli, B., 2012. Mechanical properties of defective single-layered graphene sheets via molecular dynamics simulation. Superlattices Microstruct. 51, 274–289.

Arroyo, M., Belytschko, T., 2004. Finite crystal elasticity of carbon nanotubes based on the exponential cauchy-born rule. Physical Review B 69, 115415.

Balandin, A.A., Ghosh, S., Bao, W., Calizo, I., Teweldebrhan, D., Miao, F., Lau, C.N., 2008. Superior thermal conductivity of single-layer graphene. Nano Lett. 8, 902–907.

Banhart, F., Kotakoski, J., Krasheninnikov, A.V., 2010. Structural defects in graphene. ACS Nano 5, 26–41.

Benveniste, Y., 2006. A general interface model for a three-dimensional curved thin anisotropic interphase between two anisotropic media. J. Mech. Phys. Solids 54, 708–734.

Benveniste, Y., Miloh, T., 2001. Imperfect soft and stiff interfaces in two-dimensional elasticity. Mech. Mater. 33, 309–323.

Cammarata, R., 1997. Surface and interface stress effects on interfacial and nanostructured materials. Mater. Sci. Eng. A 237, 180–184.

Cao, G., 2014. Atomistic studies of mechanical properties of graphene. Polymers 6, 2404–2432.

Dettori, R., Cadelano, E., Colombo, L., 2012. Elastic fields and moduli in defected graphene. Journal of Physics: Condensed Matter 24, 104020.

Doan, T., Le-Quang, H., To, Q.D., 2020. Effective elastic stiffness of 2d materials containing nanovoids of arbitrary shape. Int. J. Eng. Sci. 150.

Eshelby, J., 1957. The determination of the elastic field of an ellipsoidal inclusion, and related problems. Proc. R. Soc. A 241, 376–396.

Fasolino, A., Los, J., Katsnelson, M.I., 2007. Intrinsic ripples in graphene. Nature materials 6, 858–861.

Gao, Y., Hao, P., 2009. Mechanical properties of monolayer graphene under tensile and compressive loading. Physica E 41, 1561–1566.

Gibbs, J.W., 1906. The scientific papers of J. Willard Gibbs. volume 1. Longmans, Green and Company.

Gurtin, M.E., Murdoch, A., 1975. A continuum theory of elastic material surfaces. Arch. Ration. Mech. Anal 57, 291–323.

Hashin, Z., 2002. Thin interphase/imperfect interface in elasticity with application to coated fiber composites. J. Mech. Phys. Solids 50, 2509–2537.

Javvaji, B., Budarapu, P.R., Sutrakar, V., Mahapatra, D.R., Paggi, M., Zi, G., Rabczuk, T., 2016. Mechanical properties of graphene: Molecular dynamics simulations correlated to continuum based scaling laws. Comput. Mater. Sci. 125, 319–327.

Jiang, J.W., Wang, J.S., Li, B., 2010. Elastic and nonlinear stiffness of graphene: A simple approach. Phys. Rev. B 81, 073405.

Li, X., Zhang, T.Y., Su, Y., 2015. Periodically modulated size-dependent elastic properties of armchair graphene nanoribbons. Nano Lett. 15, 4883–4888.

López-Polín, G., Gómez-Navarro, C., Parente, V., Guinea, F., Katsnelson, M.I., Perez-Murano, F., Gómez-Herrero, J., 2015. Increasing the elastic modulus of graphene by controlled defect creation. Nature Physics 11, 26–31.

Los, J., Fasolino, A., Katsnelson, M., 2016. Scaling behavior and strain dependence of in-plane elastic properties of graphene. Phys. Rev. Lett. 116, 015901.

Lu, Q., Gao, W., Huang, R., 2011. Atomistic simulation and continuum modeling of graphene nanoribbons under uniaxial tension. Model. Simul. Mater. Sci. Eng 19, 054006.

Lu, Q., Huang, R., 2009. Nonlinear mechanics of single-atomic-layer graphene sheets. Int. J. Appl. Mech. 1, 443–467.

Marenić, E., Ibrahimbegovic, A., Sorić, J., Guidault, P.A., 2013. Homogenized elastic properties of graphene for small deformations. Materials 6, 3764–3782.

Memarian, F., Fereidoon, A., Ganji, M.D., 2015. Graphene Young's modulus: Molecular mechanics and DFT treatments. Superlattices Microstruct. 85, 348–356.

Milton, G.W., 2002. The theory of composites. Cambridge University Press.

Mura, T., 1987. Micromechanics of Defects in Solids. Martinus Nijhoff Publishers, Dordrecht.

Nix, W.D., Gao, H., 1998. Indentation size effects in crystalline materials: a law for strain gradient plasticity. J. Mech. Phys. Solids 46, 411–425.

Novoselov, K.S., Geim, A.K., Morozov, S.V., Jiang, D., Zhang, Y., Dubonos, S.V., Grigorieva, I.V., Firsov, A.A., 2004. Electric field effect in atomically thin carbon films. Science 306, 666–669.

Pei, Q.X., Zhang, Y.W., Shenoy, V.B., 2010. Mechanical properties of methyl functionalized graphene: a molecular dynamics study. Nanotechnology 21, 115709.

Plimpton, S., 1995. Fast parallel algorithms for short-range molecular dynamics. J. Comput. Phys. 117, 1–19.

Rafiee, R., Eskandariyun, A., 2017. Comparative study on predicting Young's modulus of graphene sheets using nano-scale continuum mechanics approach. Physica E 90, 42–48.

Reddy, C., Ramasubramaniam, A., Shenoy, V., Zhang, Y.W., 2009. Edge elastic properties of defect-free single-layer graphene sheets. Appl. Phys. Lett. 94, 101904.

Saavedra Flores, E., Ajaj, R., Adhikari, S., Dayyani, I., Friswell, M., Castro-Triguero, R., 2015. Hyperelastic tension of graphene. Appl. Phys. Lett. 106, 061901.

Savvas, D., Stefanou, G., 2018. Determination of random material properties of graphene sheets with different types of defects. Compos. B. Eng. 143, 47–54.

Scarpa, F., Adhikari, S., Phani, A.S., 2009. Effective elastic mechanical properties of single layer graphene sheets. Nanotechnology 20, 065709.

Schall, J.D., Mikulski, P.T., Ryan, K.E., Keating, P.L., Knippenberg, M.T., Harrison, J.A., 2012. Reactive empirical bond-order potentials. Encyclopedia Nanotech. , 2210–2221.

Sgouros, A., Kalosakas, G., Papagelis, K., Galiotis, C., 2018. Compressive response and buckling of graphene nanoribbons. Scientific reports 8, 1–13.

Shen, L., Shen, H.S., Zhang, C.L., 2010. Temperature-dependent elastic properties of single layer graphene sheets. Mater. Design 31, 4445–4449.

Shenoy, V., Reddy, C., Ramasubramaniam, A., Zhang, Y., 2008. Edge-stress-induced warping of graphene sheets and nanoribbons. Phys. Rev. Lett. 101, 245501.

Shuttleworth, R., 1950. The surface tension of solids. Proc. Phys. Soc 63, 444.

Terdalkar, S.S., Huang, S., Yuan, H., Rencis, J.J., Zhu, T., Zhang, S., 2010. Nanoscale fracture in graphene. Chemical Physics Letters 494, 218–222.

Torquato, S., 2001. Random heterogeneous materials: microstructure and macroscopic properties. volume 16. Springer.

Tu, Z.c., Ou-Yang, Z.c., 2002. Single-walled and multiwalled carbon nanotubes viewed as elastic tubes with the effective Young's moduli dependent on layer number. Phys. Rev. B 65, 233407.

Wang, C., Mylvaganam, K., Zhang, L., 2009. Wrinkling of monolayer graphene: a study by molecular dynamics and continuum plate theory. Phys. Rev. B 80, 155445.

Wang, S., Yang, B., Yuan, J., Si, Y., Chen, H., 2015. Large-scale molecular simulations on the mechanical response and failure behavior of a defective graphene: cases of 5–8–5 defects. Sci. Rep. 5, 14957.

Wei, X., Fragneaud, B., Marianetti, C.A., Kysar, J.W., 2009. Nonlinear elastic behavior of graphene: Ab initio calculations to continuum description. Phys. Rev. B 80, 205407.

Zhang, Y.Y., Pei, Q.X., Mai, Y.W., Gu, Y.T., 2014. Temperature and strain-rate dependent fracture strength of graphynes. Journal of Physics D 47, 425301.